
Article:
Akram, M. orcid.org/0000-0002-4427-4703, Gheit, A., Milkowski, K. et al. (2 more authors) (2025) Comparison of conventional and process intensified next generation RPB absorbers for decarbonisation of the steel industry. Fuel, 388. 134484. ISSN 0016-2361

https://doi.org/10.1016/j.fuel.2025.134484

Comparison of conventional and process intensified next generation RPB absorbers for decarbonisation of the steel industry

Muhammad Akram[1], Abdul Geit[1], Kris Milkowski[1], Willim Gale[2], Mohamed Pourkaashanian[1]

[1]Energy 2050, Translational Energy Research Centre (TERC), Department of Mechanical Engineering, University of Sheffield, Sheffield S10 2TN, UK

[2]School of Chemical and Process Engineering, University of Leeds, Leeds LS2 9JT, UK

Corresponding author:

Muhammad Akram

m.akram@sheffield.ac.uk

Abstract

This paper presents data acquired during tests carried out with the conventional Packed Bed (PB) absorber and compares with those obtained with Rotating Packed Bed (RPB) absorber. The research utilised a one Tonne per day CO_2 capture capacity PB capture plant as well as a similar capacity RPB plant, located in the Translational Energy Research Centre (TERC) at the University of Sheffield. A conventional PB stripper was used in all the tests for easy comparison of the two absorbers. Solvent used was 35% Monoethanolamine. Flue gas was generated by dosing CO_2 into air. Three sets of experiments were performed using 10%, 15% and 20% CO_2 concentrations in the flue gases and varying solvent flow rates;

1. Performance assessment of the PB absorber in combination with PB desorber to achieve 90% capture (baseline)

2. Performance assessment of the RPB absorber in combination with PB desorber under baseline conditions (same stripper conditions as in 1)
3. Performance assessment of the RPB absorber in combination with PB desorber to achieve 90% capture

It was not possible to achieve 90% capture efficiency under some conditions, due to limitation of the desorber heating system even at high reboiler duties. Optimum capture efficiency with the current design of RPB absorber was found to be ~70%. Data analysis has concluded that current design of the RPB absorber is capable to achieve 90% capture but at higher reboiler duty than the conventional plant. The limitation seems to be the residence time or insufficient contact between liquid and gas as demonstrated by low rich loadings achieved in the RPB.

However, it is important to mention here that, intensification factor defined as the ratio of packed volume of the PB absorber to that of the RPB absorber is ~14. A new RPB absorber design is proposed to achieve 90% capture efficiency under optimum conditions based on the formulae available in open literature. The proposed RPB absorber has twice the packed volume of the current RPB absorber and an intensification factor of 7.

1 Introduction

Carbon Capture, Utilisation and Storage is attracting increased attention, as awareness of the likely need for this technology in decarbonisation roadmaps grows. Without CCS, the cost of decarbonisation is expected to be £4-5bn higher per year in the 2040s [DECC, 2016]. In order to meet net zero targets by 2050, it is necessary to decarbonise the high emitting industrial sectors, of which steelmaking is one of the most important. Production of steel is growing year by year globally and demand for steel products is expected to increase from 1.89 Gt in 2020 to 3.57 Gt in 2050 in 1.5^{o} scenario [Keramidas et al. 2022]. This will increase energy consumption and CO_2 emissions [IPCC, 2021]. According to IEA

direct CO_2 emissions of crude steel production were 1.4 tonnes of CO_2 per tonne of crude steel [IEA, 2020]. CO_2 emissions can be reduced by improving energy efficiency. Also, there is an increasing trend to use electric arc furnaces in place of blast furnaces to reduce CO_2 emissions by using scrap metal. However, availability of sufficient scrap and the current inability to achieve sufficient control over scrap quality to make all grades of steel indicate that there will still be need for steel production by traditional method of blast furnace ironmaking using iron ore, followed by basic oxygen furnace steelmaking, resulting in very significant CO_2 emissions. Although it is anticipated that in the long run, hydrogen based direct reduced iron (DRI) process, in which iron ore is reduced to metallic iron in the solid state [Wei et al. 2024] will be more attractive from a carbon emission standpoint, existing blast furnaces will continue to operate for many decades in major steelmaking economies. It is anticipated that direct CO_2 emissions from steel production will be 1.1 tonnes of CO_2 per ton of crude steel [IEA, 2020]. Blast furnaces are responsible for around 70% of an integrated steel mill's CO_2 emissions [Wiley and Ho, 2011], with a CO_2 concentration ranging from 20 to 25 mol% in the flue gas [Huth and Heilos, 2013]. Therefore, CCUS technologies are required at least in the short to medium term to meet the net zero targets by 2050 by decarbonising this high emitting industry.

CCS can reduce the environmental impact of the steel industry by reducing greenhouse gas emissions. The integration of a CCS plant with a steel plant will have economic implications. The economic losses due to CCS deployment can be mitigated by sufficient cost reductions. It is expected that as the CCS technology is widely deployed, costs will reduce due to improve in technology know how and competition. Lee et al. (2022) highlighted that negative impact of CCS on steel production can be mitigated by CCS cost reduction. This will reduce the reluctance of the industry to adopt CCS.

Absorption of CO_2 using amines in packed beds is a mature and well understood technology and is used commercially. Membranes, although been used in other industries, are at very early stage of development in CO_2 capture and has some limitations such as low flux, high fouling, high-pressure requirements, and instability at extreme operating conditions. Similarly, CO_2 capture by adsorption is

also not very developed and is tested only at small scale. The process needs to be proven at larger scale before being deployed at industrial scale. Adsorbents must have high surface area, high selectivity, fast kinetics and being cost-effective. A lot of research work is going on in this filed to address these challenges but the technology in the current state is far from commercialisation. Therefore, the most attractive option in short to medium term to meet net zero targets is absorption using amines.

The technology is being used in the industry for many decades, but the use has been limited to mainly gas sweetening and manufacturing of urea. As the need for capturing CO_2 is growing from other industries, options are being explored to deploy the absorption technology to other high emitting industries. The absorption technology traditionally uses packed bed absorption columns for contacting CO_2 containing gas and absorption chemical. Aqueous amines are widely used for this application, monoethanolamine (MEA) being the baseline solvent. Heat is supplied in the desorption step to raise the temperature of the solvent to remove CO_2. Desorption uses a considerable amount of energy prohibiting widespread use of the technology. Therefore, efforts are being made to reduce costs by using alterative solvents to traditional MEA and improving energy efficiencies by integration.

As the liquid falls down through the traditional packed columns by gravity and due to the nature of slow reaction kinetics, the columns are normally very tall to provide contact time between liquid and gas. Therefore, size of a capture plant can be huge needing huge space and capital investment. For example, Lu et al. (2021) highlighted that to treat flue gas from a 960MW coal fired power plant, capture plant absorber and desorber required to be 20m dia x 64m high and 13m dia x 40m high, respectively. Efforts are being made to reduce the size of the capture plants to reduce CAPEX. One of the potential methods to achieve this is to use next generation rotating packed bed (RPB) technology [Mallinson and Ramshaw, 1981; Rao, 2022; Jassim et al, 2007]. RPBs use centrifugal force to provide mixing of liquid and gas in a shorter time. Using an RPB absorber has the potential to improve separation efficiency [Xie et al. 2019] due to increased liquid gas contact resulting in higher mass transfer [Wang et al., 2015] and a considerable drop in Height of a Transfer Unit (HTU) and is expected

96 to reduce absorber packing to 35% of a packed bed absorber volume [Chamchan et al. 2017]. The
97 smaller footprint will reduce space requirements as well as capital investment [Jiao et al. 2017]. Otitoju
98 et al. (2023) highlighted that RPBs has 3–53% lower capital expenditures as compared to packed bed
99 absorbers. Moreover, due to forced contact between liquid and gas, better absorption performance is
100 expected.

101 Practical experience for CO_2 capture by RPB_s so far has been limited to small scale. The RPB used in the
102 current study is order of magnitude bigger than the ones used so far in the open literature. Please see
103 table 1 for comparison of RPB absorber dimensions.

104 Table 1: Characteristics of RPB absorbers used for CO_2 capture

Author/s	Inner dia (mm)	Outer dia (mm)	Axial height/depth (mm)
Cheng and Tan (2009)	76	160	20
Nouroddinvand and Heidari (2021)	40	140	98
Wang et al. (2021)	50	190	23
Ma and Chen (2016)	22.5	60	18
Lin et al. (2010)	24	44	20
Theils et al. (2016)	25	125	23
Chamcham et al (2017)	120	360	60
Kang et al. (2014)	25	125	23
Jassim et al. (2007)	156	398	25
Yu et al. (2012)	76	160	20
Current study	95	1100	45

105

106 This paper presents comparison of CO_2 capture performance of a 1 Tonen Per Day (TPD) conventional
107 PB absorber with an equivalent RPB absorber at varying CO_2 concentrations and operational conditions.

Three sets of experiments are performed using 10%, 15% and 20% CO_2 containing flue gas and varying solvent flows. In all the three sets of experiments conventional PB stripper was used for direct comparison between the PB and RPB absorbers. The first set of tests was performed to establish baseline conditions with the PB absorber. In these tests, the main aim was to achieve 90% capture efficiency for all the tests at different solvent flows by varying the heat input to the reboiler. The second set of experiments was performed with the RPB absorber under similar conditions in the stripper as with the PB absorber for like for like comparison. Third set of experiments was performed to achieve 90% capture with the RPB absorber by increasing heat input to the reboiler. The data acquired for the three sets of experiments is compared as follows.

a. Performance comparison of the PB and RPB absorbers under baseline conditions
b. Performance comparison of the PB and RPB absorbers under 90% capture conditions
c. Performance comparison of the RPB absorber under baseline and 90% conditions

The experimental data was then used to calculate RPB performance parameters such as HTU, mass transfer coefficient and residence time using correlations available in open literature. Furthermore, new RPB absorber design parameters are proposed to achieve 90% capture efficiency under optimum conditions of reboiler duty.

2 Experimental facility

The overall setup used for the demonstration is shown in Figure 1. The PB CO_2 capture plant is integrated with the RPB CO_2 capture plant. Both the plants have a full absorption and desorption cycle and are integrated such that operation can be switched between the PB and RPB plants by operating the relevant valves. Moreover, it is possible to operate PB or RPB absorber in combination with either PB stripper or RPB stripper. For these tests the PB and RPB absorbers were used with PB stripper for easy comparison between the two types of absorbers. Solvent used was 35% MEA.

2.1 Description of TERC capture plant

The next generation process intensified CO_2 capture pilot scale RPB CO_2 capture plant at TERC, Figure 1, comprised of RPB absorber and RPB stripper is designed for capturing 1 TPD CO_2 based on 200 Nm^3/h gas flow having 12% CO_2. The RPB rotor has an inner diameter (D_i) of 95mm, an outer diameter (D_o) of 1.1 m and an axial depth of 45 mm packed with Montz structured packing. Average surface area of the packing is 1150 m^2/m^3 (varies from 500 – 1500 m^2/m^3) and void fraction is 0.914.

Rotational speed on the RPB absorber can go up to 800 rpm. Flue gas is fed into the RPB absorber from the circumference side at two locations at 180 deg. The flue gas flow inwards and leaves from the centre. Solvent is fed from the centre and flows outwards and leaves from the bottom of the absorber as the absorber is orientated vertically (axis of rotation are horizontal) as shown in Figure 1. Table 2 provides characteristics of the PB and RPB absorbers. The RPB absorber packed volume is 14 times smaller than the PB absorber.

The RPB plant is integrated with the PB plant. The PB is equipped with a cross exchanger, a carbon filter and a water wash. The PB absorbers, two of them, are packed with 6m of Flexipac structured packing (from Koch Glitsch) each with liquid distribution at the top and middle of the column. The PB stripper is packed with IMTP25 random packing from Koch Glitsch.

Most of the infrastructure is shared between the two plants. The PB stripper uses pressurised hot water (PHW) to desorb CO_2. The flow rate of PHW and temperature can be changed to achieve different capture efficiencies. Reboiler duty for PB reboiler is calculated by measuring PHW flow rate and its inlet and outlet temperatures to the reboiler.

There are four possible combinations in which integrated PB and RPB plants can be operated.

1. PB absorber + PB stripper
2. RPB absorber + PB stripper

3. PB absorber + RPB stripper
4. RPB absorber + RPB stripper

The switching between any mode of operation is by adjusting the relevant valve positions. For all the tests reported here, first two modes of operation were used.

Figure 1

Table 2: Packed volume of PB and RPB absorbers

PB			RPB					
packed height	dia	packed volume	Outer dia (Do)	Inner dia (Di)	Depth (z)	Packed volume	V_{RPB} as %age of V_{PB}	Intensification factor V_{PB}/V_{RPB}
m	m	m^3	m	m	m	m^3		
12	0.25	0.589	1.1	0.095	0.045	0.042	7.2	13.9

2.2 Measurements and calculation:

Following measurements were recorded during the tests.

- Temperature, flow and pressure measurements at various locations on the CO_2 capture plant
- PHW flow and temperature measurements for reboiler duty calculations
- Gaseous compositions at absorber inlet and outlet were measured using Gasmet FTIR for capture efficiency calculations
- Solvent samples were analysed using Mettler Toledo for solvent concentration and CO_2 loadings

Based on the analytical measurements and plant operational data capture efficiency, reboiler duty and CO_2 loadings have been calculated using the formulae previously presented in Akram et al. (2016).

2.2.1 Gasmet DX4000 FTIR:

The Gasmet DX4000 FTIR was used for gas analysis, which can sequentially test samples from different locations of the plant. The sequence and sampling time is user defined and can be changed in the FTIR software as and when required. For these tests, gas compositions at absorber inlet and outlet were used for capture efficiency calculations. The sampling points are common for both the PB and RPB plants.

The gas samples are extracted from the plant using isokinetic sampling probes and routed to the FTIR through heated filters, heated sampling lines and a heated cabinet housing solenoids for sample switching. The entire sampling system is heated up to 180 ^{o}C to avoid condensation.

2.2.2 Mettler Toledo auto-titrator:

Solvent analyses were performed by Mettler Toledo auto-titrator, T9. For these tests, rich and lean solvents samples were collected directly from the plant and analysed manually using the titrator for MEA concentration and CO_2 loadings.

3 Experimental matrix:

The experimental matrix was designed based on a modelling study designed to test steel industry gas compositions in the PB. To expand the study for wider applicability, three different CO_2 concentrations (20% ,15%, 10%) were investigated, 20% being representative of steel industry flue gases. Experimental matrix is shown in the Table 2. Tests were first conducted with the PB absorber to establish baseline conditions. In the rest of the paper tests with the PB absorber will be referred to

as “baseline conditions”. All the tests reported here were conducted with synthetic flue gas, mixture of air and CO_2.

During the baseline tests heat input to the reboiler was varied to achieve 90% capture at different solvent flow rates (L/G ratios). The heat input to the reboiler was varied by varying PHW temperature set point. At least five solvent flow rates were investigated at each CO_2 concentration. Stripper pressure for all the tests was maintained at 20 kPa. Flue gas flow was maintained at 150 m^3/h.

Following the baseline tests, two sets of tests were performed with the RPB absorber at every solvent flow rate tested in the baseline case, with some exceptions at the lower solvent flow at 10% CO_2, please see Table 3. First set of tests with the RPB absorber was performed under baseline conditions in the stripper for comparison between the PB absorber performance to that of the RPB absorber. The plant was allowed to get to steady state to establish capture efficiency and reboiler duty differences between PB and RPB absorbers under similar operational conditions. The second set of tests with the RPB absorber was performed to try to achieve 90% capture to compare reboiler duties for the two types of absorbers. For these tests PHW set point was gradually increased to achieve ~90% capture. It was not possible to achieve 90% capture with RPB absorber at 20% CO_2 due to PHW operational temperature limitation (125 ^oC max) so the PHW set point was set to 125 ^oC and the plant was allowed to get to steady state.

Table 3: Experimental matrix

	Solvent flow (kg/h)				Solvent flow (kg/h)		
CO_2 conc.	PB absorber	RPB absorber	RPB absorber	CO_2 conc.	PB	RPB absorber	RPB absorber
	90% capture (baseline)	Baseline	90% capture		90% capture (baseline)	Baseline	90% capture
10%	500	500	500	15%	600	600	600
	400	400	400		700	700	700

	600	600	600		800	800	800
	700	700	700		900	900	900
	300	300	450		500	500	500
	350	-	-				
	800	800	800				
	900	900	900				
20%	1000	1000	1000				
	1100	1100	1100				
	1200	1200	1200				

4 Results and discussion:

The results for the three test campaigns are compared in the following sections.

The data presented here has some fluctuations. The data is affected by various factors such as instrument accuracies, human errors, weather, size of the equipment. Due to the pilot scale nature of the facility and being located outside in open atmosphere, atmospheric conditions have an impact on the data. The tests were carried out during 24 hr operation resulting in variation in atmospheric conditions which has in turn resulting in data fluctuations.

4.1 RPB and PB absorbers comparison under baseline conditions:

4.1.1 Capture efficiency and reboiler duty:

The performance of the RPB absorber under baseline conditions is compared with the PB absorber in Figures 2-4 at 10%, 15% and 20% CO_2, respectively.

It can be observed from the data that capture efficiency with the RPB absorber at 10% CO_2, Figure 2, is always lower than that with the PB absorber but the reboiler duty is always higher except for one condition i.e. 300 kg/h solvent flow. The operation in this range should be avoided as the reboiler duty with the PB absorber observed to increase exponentially at solvent flow below 400 kg/h. Reboiler duty with the PB absorber at 300 kg/h solvent flow is 6.57 MJ/kg which is ~75% higher than the minimum 3.76 MJ/kg achieved with the PB absorber at 10% CO_2. Another way to look at it is that the reboiler duty of 4.58 MJ/kg with the RPB absorber is ~14% higher than the minimum achieved with the RPB absorber at 10% CO_2. The figure shows that at 400 kg/h solvent flow, the boiler duty with the RPB absorber is marginally higher but the capture efficiency is considerably lower than that with the PB absorber. This also highlights that at 300 kg/h solvent flow, residence time of the solvent in the RPB absorber is higher as compared to that at 400 kg/h and thus was able to achieve 80% capture efficiency.

The reboiler duty has shown a similar trend for both absorbers and minimum reboiler duty at 10% CO_2 for both is achieved at 400-500 kg/h solvent flow. At 500 kg/h solvent flow capture efficiency is 18% lower while reboiler duty is 7% higher with the RPB absorber than that with the PB absorber. Beyond 500 kg/h solvent flow, trend is increasing reboiler duty and decreasing capture efficiency with the RPB absorber.

As solvent flow rate is increased reboiler duty first decreases then increases. During these tests reboiler temperature was varied to achieve 90% capture for the PB absorber. The temperature was lowered as solvent flow was increased. Lower reboiler temperature results in higher lean loading. Increase in solvent flow also decreases residence time in the reboiler resulting in increased lean loading. However, higher solvent flow also means that more energy is required to heat up the solvent in the reboiler. Therefore, there are a number of factors affecting the reboiler duty. The effect of all these factors is optimum at the minimum reboiler duty.

Figure 2:

Figures 3 compares the capture effciency and reboiler duty obtained with the RPB absorber to that with the PB absorber at 15% CO_2. As can be observed from the figure that the capture efficnecy was always lower with the RPB absorber and kept decreasing with increase in the solvent flow rate. During the baseline test=s with PB absorber with increase in solvent flow, PHW setpoint was decreased to achieve 90% capture. The same PHW setpoint parameters were then repeated with the RPB absorber and decrease in PHW setpoint resulted in drop in capture efficiency. At 500 kg/h solvent flow, the capture effciency with the RPB absorber is 12% lower while at 900 kg/h solvent flow it is ~33% lower. On the other hand reboiler duty was almost similar at 500 and 600 kg/h solvent flow but was ~20% higher at higher solvent flow rates. Again, reboiler duty has shown similar trend for both types of absorbers. It is worth noting that capture effciency with the RPB absorber was the highest, at the lowest solvent flow rate, 500 kg/h. This justified the argument that at higher residence time, capture efficiency is higher. Therfore, in order to achive 90% capture under optimum conditions, residence time has to be incerased, please see section 4.4 for further discussions on this topic.

Figure 3:

Figures 4 compares the captrue efficiency and reboiler duty obtained for the two absorbers at 20% CO_2. As can be observed from the Figure that for all the cases investigated, the reboiler duty is 12-18% higher while the capture efficiency is 25-30% lower with the RPB absorber as compared to that with the PB absorber. Higher reboiler duty with the RPB absorber, although stripper conditions were the same, is to some extent due to lower capture efficiency with the PRB absorebr as the total amount of CO_2 captured is lower.

Figure 4:

4.1.2 CO_2 loadings:

Figures 5-7 compare rich loading, lean loading and solvent capacity obtained with the RPB absorber to those with the PB absorber under the baseline conditions at 10%, 15% and 20% CO_2

concentrations, respectively. Rich and lean loadings represent CO_2 content in the rich and lean solvent streams, respectively, as moles of CO_2 per mole of MEA. Solvent capacity is the difference between the rich and lean loadings. It can be observed from the figures that lean loadings for the two types of absorbers are not much different as stripper conditions were the same. However, rich loadings are considerably lower with the RPB absorber than with the PB absorber under similar conditions.

The figures indicate that the rich loading is 17-38% lower while the solvent capacity is 23-52% lower with the RPB absorber than with the PB absorber. Also, difference in rich loading drops with increase in the CO_2 concentration due to the higher amount of CO_2 available. However, rich loadings were still considerably lower with the RPB absorber as compared to those with the PB absorber indicating that solvent was not loaded to its full extent in the case of RPB absorber due to insufficient residence time.

Figure 5:

Figure 6:

Figure 7:

4.2 RPB and PB absorbers comparison under 90% capture conditions:

4.2.1 Reboiler duty and capture efficiency:

The performance of the RPB absorber under 90% capture conditions is compared with the PB absorber in Figures 8-10 at 10%, 15% and 20% CO_2, respectively.

It can be observed from the data that it was possible to achieve 90% capture with the RPB absorber at 10% and 15% CO_2 (except at 500kg/h solvent flow) but was not possible at 20% CO_2 due to limitation in the heat input to the reboiler.

At 10% CO_2, Figure 8, reboiler duty with the RPB absorber has similar trend but is higher than that with the PB absorber. With the PB absorber minimum reboiler duty at 10% CO_2 is 3.76 MJ/kg while

307 with the RPB absorber is 6.4 MJ/kg (70% higher). The figure shows that the reboiler duty with the
308 RPB absorber is considerably higher than that with the PB absorber, ranging from 46% at higher
309 solvent flows to 134% at lower solvent flows. The difference in the reboiler duty appears to be
310 dropping with increase in solvent flow, but the drop is flattening as solvent flow is further increased.

311 Figure 8

312 At 15% CO_2, Figures 9, trend in reboiler duty is similar with both types of the absorbers. However,
313 reboiler duty is 45% to 65% higher with the RPB absorber as compared to that with the PB absorber.
314 As observed above at 10% CO_2, the difference between the reboiler duty has slightly decreasing
315 trend with increase in the solvent flow rate.

316 Figure 9

317 It was not to achieve 90% capture with the RPB absorber at 20% CO_2. However, general trend is that
318 the capture efficiency increased with increase in the solvent flow ranging from 81% at 800 kg/h to
319 86% at 1200 kg/h, Figure 10. In these tests PHW set point was kept at 125 ^{o}C, maximum permissible,
320 thus increase in solvent flow resulted in higher capture efficiency due to the availability of higher
321 amount of the solvent to capture more CO_2.

322 Reboiler duty with the RPB absorber was 19% to 36% higher as compared to that with the PB
323 absorber. In future, new PHW system which can be operated at up to 150 ^{o}C will allow the reboiler
324 operation at higher temperatures so it may be possible to achieve 90% capture with the RPB
325 absorber at 20% CO_2 but it is expected that reboiler duty will increase further.

326 Figure 10

327 ### 4.2.2 CO_2 loadings:

328 Figures 11-13 compare rich loading, lean loading and solvent capacity obtained with the RPB
329 absorber to those with the PB absorber under 90% capture (125 ^{o}C in the case of 20% CO_2 with RPB
330 absorber) conditions at 10%, 15% and 20% CO_2 concentrations. Some of the tests were performed

during night operation or weekends by controlling the plant remotely, loadings data for these tests is not available. It can be observed from the figures that both rich and lean loadings are considerably lower with the RPB absorber than with the PB absorber under 90% capture conditions. However, in this case difference in the solvent capacities between the two modes of operation is much smaller than the baseline conditions.

The figures indicate that rich loading is 20-36% lower, lean loading is 28-43% lower while solvent capacity is 6-31% lower with the RPB absorber than with the PB absorber. Considerably lean loadings with RPB absorber in these tests highlight that in order to achieve 90% capture efficiency, more energy was input to the reboiler to make the solvent leaner and thus higher reboiler duties. Also, the difference in the rich loading drops with increase in CO_2 concentration due to the higher amount of CO_2 available.

Figure 11

Figure 12

Figure 13

4.3 RPB absorber comparison under baseline and 90% capture conditions:

4.3.1 Capture efficiency and reboiler duty:

Figures 14-16 compare the performance of the RPB absorber under the baseline and 90% capture (125 ^{o}C at 20% CO_2) conditions at 10%, 15% and 20% CO_2 concentrations. The figures plot percentage increase in the capture efficiency and the reboiler duty under 90% capture conditions with respect to the baseline conditions. The figures show that there is a general trend, with some slight deviations, that percentage increase in the capture efficiency is increasing while that in the reboiler duty is decreasing as solvent flow rate is increased at 10% and 15% CO_2 concentrations. However, in the case of 20% CO_2 concentration, percentage increase in reboiler duty first decrease then increases as

355 solvent flow is further increased. The maximum solvent flow in the current PB absorber is limited to
356 1200 kg/h due to distributor design limitations. Therefore, it is not possible to test higher solvent
357 flows without significant investment in redesigning and replacing all the four distributors.

358 Figure 14

359 Figure 15

360 Figure 16

361 ### 4.3.2 CO_2 loadings:

362 Figures 17-19 compare CO_2 loadings with the RPB absorber under the baseline and 90% capture (125
363 ^{o}C at 20% CO_2) conditions at 10%, 15% CO_2 and 20% CO_2 concentrations. It can be observed from
364 Figure 17 that rich loadings are similar under both cases at 10% CO_2 while lean loadings are
365 considerably lower under 90% capture conditions. At 15% CO_2, rich loadings are similar at low
366 solvent flows while are lower for 90% capture at higher solvent flows. Figure 18 indicates that rich
367 loading varies from 11% higher to 17% lower while lean loading is 14-42% lower under 90% capture
368 conditions as compared to that under the baseline conditions. The gap between the rich and lean
369 loadings widens as the solvent flow is increased. However, in the case of 20% CO_2, the gap between
370 the rich and lean loading is almost consistent. The figure 19 indicates that rich loading is 4-14% lower
371 while lean loading is 23-30% lower under 125 ^{o}C conditions as compared to the baseline.

372 It is evident that higher energy is required to get lower lean loadings to capture 90% CO_2 with the
373 RPB absorber under those conditions. Therefore, by analysing the RPB absorber data for capture
374 efficiency and reboiler duty at 10% and 50% CO_2 concentrations, it can be concluded that the
375 optimum conditions of minimum reboiler duty for the current design of the RPB absorber in
376 combination with PB stripper is ~70% capture efficiency. The current standard for capture efficiency
377 for the new build capture plants is 90-95%. Therefore, in order to meet the best practice capture
378 efficiency requirements, RPB absorber needs to be redesigned to provide more residence time to

provide sufficient contact between the liquid and gas streams. Rotational speed is expected to have an impact on the capture efficiency, but no appreciable difference was observed at difference rotational speeds for the RPB. Flow pattern in the RPB can be improved or different packing can be used to provide more residence time.

The RPB absorber is driven by a 4.7 KW motor. For these tests the RPB was operated at 600 rpm which is 75% of the full speed. The power consumption by the motor was not directly measured but can be roughly estimated by calculations. The calculated electricity usage by the motor at 75% of the rated capacity is 1.98 kW (7.1 MJ/h). This increases energy consumption (reboiler duty + motor consumption) by 2.7 to 8% depending upon the reboiler duty. Higher the reboiler duty, lower the percentage increase due to motor consumption. At optimum reboiler duty of 3.7 MJ/kg, motor consumption increases the total energy consumption by 5.8%.

Figure 17

Figure 18

Figure 19

4.4 Comparison of PB and RPB absorbers by Transfer unit:

The discussions in the above section indicate that, for similar operational conditions, the RPB absorber has not performed as well as the PB absorber as the capture efficiency with the RPB absorber for all the baseline conditions tested was lower than that with the PB absorber. It was possible to achieve 90% capture with the RPB absorber but at the cost of higher reboiler duty. However, it should be noted that the RPB absorber is much smaller than the PB absorber. The packed volume of the RPB absorber is ~7% of the PB absorber packed volume, see Table 2. While intensification factor defined by, the ratio of packed volume of the PB absorber to the packed volume of the RPB absorber, is 14.

An alternative RPB absorber design is required which can achieve 90% capture efficiency under optimum conditions. Agarwal et al. (2010) described design procedure for RPB absorbers and highlighted that an RPB absorber should be designed to provide sufficient contact between liquid and gas. In the following section, using the correlations available in open literature, a new RPB absorber design to achieve 90% capture efficiency under optimum conditions is proposed.

The scientific way to compare the performance of an absorption systems is by calculating the Height of a Transfer Unit (HTU). Mass transfer from one phase to the other depends upon fluid motion and hydrodynamic characteristics [Shukla et al. 2023]. Agarwal et al. (2010) while describing RPB absorber design procedures for CO_2 capture applications highlighted that the HTU depends upon mass transfer coefficients which are dependent upon RPB design and packing type and thus should be determined experimentally for a specific system. For the current RPB, under the experimental conditions tested, gas phase overall mass transfer coefficient has been calculated by using equation 1 [Jassim et al. 2007; Kolawole, 2019].

$$K_G a_e = \frac{Q_G}{\pi(r_o^2 - r_i^2)z} \ln\left(\frac{y_i}{y_o}\right) \quad (1)$$

Liquid residence time in an RPB is related to liquid hold up defined as the ratio of liquid volume to packing volume [Xie et al., 2017]. Liquid residence time in the RPB absorber is calculated by using equation 2 [Burns et al. 2000].

$$t_{res} = \frac{\varepsilon_L \pi(r_o^2 - r_i^2)}{u_o d} \quad (2)$$

Correlation for HTU calculation for PB and RPB absorbers proposed by Chamchan et al. (2017) and Kolawole, (2019), respectively, are presented in equations 3 and 4.

$$HTU_{PB} = \frac{H_{PB}}{\ln\frac{Y_i}{Y_O}} \quad (3)$$

425 $$HTU_{RPB} = \frac{r_O - r_i}{ln\frac{y_i}{y_O}}$$ 4

426 Where:

427 d = width of the solvent injection nozzle (m)

428 ε_L = Liquid hold up in RPB absorber

429 H_{PB} = Packed height of PB absorber (m)

430 HTU_{PB} = Height of a Transfer Unit in PB absorber

431 HTU_{RPB} = Height of a transfer unit in RPB absorber

432 $K_G a_e$ = Overall gas phase mass transfer coefficient (1/s)

433 Q_G = Gas volumetric flow rate (m^3/h)

434 r_i = Inner radius of the RPB absorber (m)

435 r_o = Outer radius of the RPB absorber (m)

436 t_{res} = Residence time in RPB (s)

437 u_o = Liquid jet velocity through the solvent injection nozzle (m/s)

438 y_i = CO_2 %age at absorber inlet

439 y_o = CO_2 %age at absorber outlet

440 z = axial depth of the RPB absorber (m)

441 The formula used by Kolawole (2019) for HTU calculation for a RPB based on radius does not
442 consider cross-sectional area and thus does not take into account the polar coordinates. Otitoju et al.
443 (2023) proposed the use of area of a transfer unit (ATU) instead of HTU to address the issue of polar
444 coordinates. They validated their model using pilot scale RPB experimental data from Jassim et al.
445 (2007). The pilot scale PRB had an inner dia of 156mm, outer dia of 396mm and axial height of

446 0.025m. The model was then used to design a scaled up RPB for a 250 MWe CCGT power plant.
447 Packed volume of the pilot scale RPB used for the model validation was 0.0026 m^3 while that of the
448 scaled up RPB was 21 m^3, a scale up factor of ~8000 on packed volume basis. They used an iterative
449 process using empirical equations to calculate dimensions of the RPB absorber required to capture
450 CO_2 from the CCGT plant. The ATU was calculated by using equation 5.

451 $$ATU = \frac{F_g}{ZK_{tot}P} \quad (5)$$

452 Where;

453 K_{tot} = Overall gas phase mass transfer coefficient

454 F_g = Molar gas flow

455 P = Overall pressure

456 They then calculated radius of the scaled up RPB using equation 6.

457 $$r_o = \sqrt{\frac{ATU*NTU}{\pi} + r_i^2} \quad (6)$$

458 Where, NTU is the number of transfer units defined by equation 7;

459 $$NTU = \ln\frac{y_i}{y_o} \quad (7)$$

460 The current study is mainly focussed on comparison between PB and RPB absorbers. As it is not
461 possible to calculate ATU for the PB absorber due to cylindrical shape, a new term Volume of a
462 Transfer unit (VTU) is introduced by considering axial height of the RPB. The equation 6 is modified to
463 replace ATU with VTU.

464 $$r_o = \sqrt{\frac{VTU*NTU}{\pi z} + r_i^2} \quad (8)$$

465 The data analysis in the previous sections have revealed that the current RPB absorber has optimum
466 capture efficiency of ~70% due to short contact time. Therefore, a slightly bigger RPB absorber is

467 required to achieve 90% capture at optimum conditions. Equation 8 can be rearranged to calculate
468 VTU for the experimental conditions.

469 $$VTU = \frac{r_o^2 - r_i^2}{NTU}\pi Z \quad (9)$$

470 NTU is related to capture efficiency and is calculated by using equation 7, equation 9 is then used to
471 calculate VTU for all the experimental conditions tested.

472 Inner radius and axial height (width) of an RPB absorber are determined by gas throughput while
473 outer radius is determined by the desired separation efficiency [Agarwal et al. 2010; Hacking et al.
474 2020]. As the aim here is to design a new RPB absorber to achieve higher (90%) capture for the
475 same experimental conditions, inner radius and width are not changed in this case. For 90% capture
476 efficiency NTU is equal to 2.3. Equation 8 is used to calculate the new outer radius required to
477 achieve 90% capture under the operational conditions. The calculated results using the above
478 equations are presented and discussed in the following section.

479 Figure 20 plots overall gas phase mass transfer coefficient vs solvent flow for the bassline conditions.
480 The plot indicates that the mass transfer coefficient has slightly decreasing trend with increase in the
481 solvent flow due to decrease in residence time as solvent flow is increased.

482 Figure 20

483 Figure 21

484 Figure 21 plots the capture efficiency achieved under the experimental conditions vs. VTU and the
485 overall mass transfer coefficient for the RPB under the baseline and the 90% (or 125 ^{o}C) capture
486 conditions. It can be observed from the plot that the mass transfer coefficient has a direct
487 relationship while the VTU has an inverse relationship with the capture efficiency.

488 Figure 22

Based on the VTU values it is possible to calculate the new RPB outer radius to achieve 90% capture efficiency under the similar conditions assuming that VTU for a particular set of conditions remains the same. The new outer radius can then be used to calculate required packed volume of RPB as a percentage of packed volume of PB.

Figure 22 plots residence time of the current absorber and the proposed new design vs. solvent flow. The plot shows that residence time reduces with increase in solvent flow as expected. Residence time in the new proposed RPB design to achieve 90% capture is 1.2 to 1.5 times higher than the current RPB over the range of the solvent flows presented.

Figure 22

Figure 23 plots required RPB radius vs achieved capture efficiency. The figure also plots capture efficiency vs intensification factor, the ratio of packed volume of the PB absorber to that of the RPB absorber. It can be observed from the figure that at the conditions with optimum reboiler duty (~70% capture efficiency) intensification factor is ~7. Therefore, a new design of the RPB absorber with a packed volume twice the packed volume of the current RPB absorber and 14% of that of the PB absorber can achieve 90% capture with optimum reboiler duty. The ratio of the residence time in the new RPB absorber to that of the exiting RPB will be 1.4. This is in line with RPB design presented by Agarwal et al. (2010) who also reported 7 times volume reduction factor for RPB absorber compared to PB absorber. The proposed design would be better than that assessed by Im et al. (2020) who reported that RPB absorber with 3 times less volume can capture the same amount (90%) of CO_2 as the PB absorber.

Figure 23

5 Conclusions:

Three sets of experiments have been performed at varying CO_2 concentrations and solvent flows. CO_2 concentrations tested are 10%, 15% and 20%. Conventional packed bed absorber and stripper

performance is assessed at different conditions (baseline) to achieve 90% capture efficiency. Performance of RPB and conventional stripper is assessed under baseline conditions followed by 90% capture conditions. Following conclusions can be drawn from the data.

- Under similar conditions, capture efficiency with the current RPB absorber, having 7% packed volume of the PB absorber, is lower while reboiler duty is higher as compared to that with the PB absorber
- It is possible to achieve 90% capture with the current RPB absorber but at the cost of higher energy penalty.
- Optimum capture efficiency with the current design seems to be ~70%
- Rich loadings obtained with the RPB absorber are lower than those obtained with the PB absorber indicating that there is not enough residence time to fully load the solvent
- Lean loadings with the RPB and PB absorbers are similar under baseline conditions while are considerably lower with the RPB absorber under 90% capture conditions. Therefore, more energy is required to strip the solvent to achieve 90% capture in the case of the RPB absorber.
- Main issue with the RPB absorber seems to be the residence time or insufficient contact to fully load the solvent.
- A new design for RPB absorber is proposed to achieve 90% capture under optimum conditions. The new absorber has an outer radius of ~1.6m and twice the packed volume of the current RPB absorber and 14% the packed volume of the PB absorber and an intensification factor of 7. Residence time in the new RPB absorber will be increased to 1.4 times the current RPB absorber.

There is currently very limited experimental data available in open literature on CO_2 capture from steel industry. This article presented CO_2 capture data from flue gas representing steel industry CO_2 gas concentrations. The flue gas used in this study was CO_2 doped air which does not

represent potential contaminants in the steel industry flue gases. However, for the parameters presented in the paper such as capture efficiency, reboiler duty and CO_2 loadings, contaminants presence is not of much relevance. The contaminants can affect the solvent performance in the long term by degradation. This aspect will be investigated in future studies.

6 Acknowledgement

The authors want to acknowledge the financial support provided by the Centre for Research into Energy Demand Solutions (CREDS). Experimental facilities of the Translational Energy Research Centre (TERC) at the University of Sheffield, funded by European Regional Development Fund (ERDF) and Department for Energy Security and Net Zero (DESNZ) have been used for the experimental work.

7 References:

- Agarwal, L., Pavani, V., Rao, D.P. and Kaistha, N. (2010) 'Process Intensification in HiGee Absorption and Distillation: Design Procedure and Applications', *Industrial & Engineering Chemistry Research*, 49(20), pp. 10046-10058.
- Akram, M., Ali, U., Best, T., Blakey, S., Finney, KN., Pourkashanian M., (2016), Performance evaluation of PACT Pilot-plant for CO_2 capture from gas turbines with Exhaust Gas Recycle, International Journal of Greenhouse Gas Control Volume 47, April 2016, Pages 137-150
- Burns, R.J., Jamil, J.N., and Ramshaw, C., 2000, Process intensification: operating characteristics of rotating packed beds - determination of liquid hold-up for a high-voidage structured packing, Chemical Engineering Science 55 (2000) 2401-2415
- Chamchan, N., Chang, J. Y., Hsu, H. C., Kang, J. L., Wong, D. S. H., Jang, S. S., et al. (2017). Comparison of rotating packed bed and packed bed absorber in pilot plant and model simulation for CO_2 capture. J. Taiwan Inst. Chem. Eng. 73, 20–26. doi:10.1016/j.jtice.2016.08.046

562 • Cheng, H.-H. and Tan, C.-S. (2009) 'Carbon dioxide capture by blended alkanolamines in
563 rotating packed bed', Energy Procedia, 1(1), pp. 925-932.
564 • DECC, A strategic approach to carbon capture and storage, Committee on Climate Change,
565 Letter to DECC Secretary of State, 6th July, 2016
566 • Gibbins J. Amine stripper temperature profile a key to optimising net-zero performance in
567 post-combustion carbon capture plants | LinkedIn. LinkedIn 2023.
568 https://www.linkedin.com/pulse/amine-stripper-temperature-profile-key-optimising-net-
569 zero-gibbins/ (accessed January 28, 2024).
570 • Hacking, J. A. et al. 2020, Improving liquid distribution in a rotating packed bed, Chemical
571 Engineering & Processing: Process Intensification 149 (2020) 107861
572 • Huth M, Heilos A. 14 - Fuel flexibility in gas turbine systems: impact on burner design and
573 performance. In: Jansohn P, editor. Modern Gas Turbine Systems, Woodhead Publishing;
574 2013, p. 635–84. https://doi.org/10.1533/9780857096067.3.635.
575 • IEA, 2020, Iron and Steel Technology Roadmap, Towards more sustainable steelmaking, Part
576 of the Energy Technology Perspectives series
577 • Im D, Jung H, Lee JH. Modeling, simulation and optimization of the rotating packed bed (RPB)
578 absorber and stripper for MEA-based carbon capture. Comput Chem Eng 2020;143:107102
579 • IPCC, 2021: Climate Change 2021: The Physical Science Basis. Contribution of Working Group
580 I to the Sixth Assessment Report of the Intergovernmental Panel on Climate Change, 2021.
581 • Jassim, M.S., Rochelle, G., Eimer, D. and Ramshaw, C. (2007) 'Carbon Dioxide Absorption and
582 Desorption in Aqueous Monoethanolamine Solutions in a Rotating Packed Bed', *Industrial &*
583 *Engineering Chemistry Research*, 46(9), pp. 2823-2833.
584 • Jiao, W., Luo, S., He, Z. and Liu, Y. (2017) 'Applications of high gravity technologies for
585 wastewater treatment: A review', Chemical Engineering Journal, 313, pp. 912-927.
586 • Keramidas, K., Fosse, F., Diaz Rincon, A., Dowling, P., Garaffa, R., Ordonez, J., Russ, P., Schade,
587 B., Schmitz, A., Soria Ramirez, A., Vandyck, T., Weitzel, M., Global Energy and Climate Outlook

588 2022: Energy trade in a decarbonised world, Publications Office of the European Union,
589 Luxembourg, 2022, doi:10.2760/863694, JRC131864
590 • Keyvani, M. and Gardner, N.C. (1989) 'Operating characteristics of rotating packed beds',
591 Chemical Engineering Progress September, pp. 48-52.
592 • Kolawole T.O. (2019) Intensified Post-Combustion Carbon Capture using a Pilot Scale Rotating
593 Packed Bed and Monoethanolamine Solutions, PhD thesis, Newcastle University, UK
594 • Lin, C.-C., Lin, Y.-H. and Tan, C.-S. (2010) 'Evaluation of alkanolamine solutions for carbon
595 dioxide removal in cross-flow rotating packed beds', Journal of Hazardous Materials, 175(1),
596 pp. 344-351.
597 • Lu S., Fang M., Li Q., et al. The experience in the research and design of a 2 million tons/year
598 flue gas CO_2 capture project for coal-fired power plants, International Journal of Greenhouse
599 Gas Control, 110 (2021) 103423
600 • Ma, H. J., and Chen, Y. S. (2016). Evaluation of effectiveness of highly concentrated
601 alkanolamine solutions for capturing CO_2 in a rotating packed bed. Int. J. Greenh. Gas Control
602 55, 55–59. doi:10.1016/j.ijggc.2016.11.009
603 • Mallinson, R. H., and Ramshaw, C. (1981). Mass transfer process. Patent No. 4,283,255.
604 United States: United States Patent.
605 • Michailos S, Gibbins J. A Modelling Study of Post-Combustion Capture Plant Process
606 Conditions to Facilitate 95–99% CO_2 Capture Levels from Gas Turbine Flue Gases. Frontiers in
607 Energy Research 2022;10.
608 • Michailos S, Gibbins J. Effect of stripper pressure and low lean loadings on the performance
609 of a PCC plant for 99% CO_2 capture level. SSRN Electronic Journal 2022.
610 https://doi.org/10.2139/ssrn.4283827.
611 • Norizam N.N.A.N. et al. (2024), Impact of the blending of kaolin on particulate matter (PM)
612 emissions in a biomass field-scale 250 kW grate boiler, Fuel 374 (2024) 132454.

- Nouroddinvand, V.M., and Heidari, A. (2021). Experimental study of CO_2 absorption with MEA solution in a novel Arc-RPB. Chem. Eng. Process. – Process Intensif. 165, 108450. doi:10.1016/j.cep.2021.108450
- Otitoju, O., Oko, E., Wang, M., (2023), Modelling, scale-up and techno-economic assessment of rotating packed bed absorber for CO_2 capture from a 250 MWe combined cycle gas turbine power plant, Applied Energy 335 (2023) 120747
- Rao, D. P. (2022). Commentary: Evolution of high gravity (HiGee) technology. Ind. Eng. Chem. Res. 2022, 61, 997−1003.
- Shukla C, Mishra P and Dash SK (2023), A review of process intensified CO_2 capture in RPB for sustainability and contribution to industrial net zero. Front. Energy Res. 11:1135188. doi: 10.3389/fenrg.2023.1135188
- Theils, M., et al. (2016), Modelling and Design of Carbon Dioxide Absorption in Rotating Packed Bed and Packed Column, IFAC-PapersOnLine 49-7 (2016) 895–900
- Wang, M., Joel, A.S., Ramshaw, C., Eimer, D. and Musa, N.M. (2015) 'Process intensification for post-combustion CO_2 capture with chemical absorption: A critical review', Applied Energy, 158, pp. 275-291.
- Wang, Y., Dong, Y., Zhang, L., Chu, G., Zou, H., Sun, B., et al. (2021). Carbon dioxide capture by non-aqueous blend in rotating packed bed reactor: Absorption and desorption investigation. Sep. Purif. Technol. 269, 118714. doi:10.1016/j.seppur.2021.118714
- Wei C., Zhang X., Zhang J., Xu L., Li G., Jiang T., (2024), Development of Direct Reduced Iron in China: Challenges and Pathways, Engineering, https://doi.org/10.1016/j.eng.2024.04.025
- Weiland R, Hatcher N, Alvis S. Pinched Performance: Part 1. Digital Refining 2015.
- Wiley DE, Ho MT, Bustamante A. Assessment of opportunities for CO_2 capture at iron and steel mills: An Australian perspective. Energy Procedia 2011;4:2654–61. https://doi.org/10.1016/j.egypro.2011.02.165.

- Xie, P., Lu, X., Ding, H., Yang, X., Ingham, D., Ma, L. and Pourkashanian, M. (2019) 'A mesoscale 3D CFD analysis of the liquid flow in a rotating packed bed', *Chemical Engineering Science*, 199, pp. 528-545.
- Xie, P., Lu, X., Yang, X., Ingham, D., Ma, L. and Pourkashanian, M. (2017) 'Characteristics of liquid flow in a rotating packed bed for CO_2 capture: A CFD analysis', *Chemical Engineering Science*, 172, pp. 216-229.
- Yu C.H., Cheng, H.H., Tan C.S., (2012), CO_2 capture by alkanolamine solutions containing diethylenetriamine and piperazine in a rotating packed bed, Int. J. Greenhouse Gas Control, 9 (2012), pp. 136-147
- Zhao, B., Tao, W., Zhong, M., Su, Y. and Cui, G. (2016) 'Process, performance and modelling of CO_2 capture by chemical absorption using high gravity: A review', Renewable and Sustainable Energy Reviews, 65, pp. 44-56.

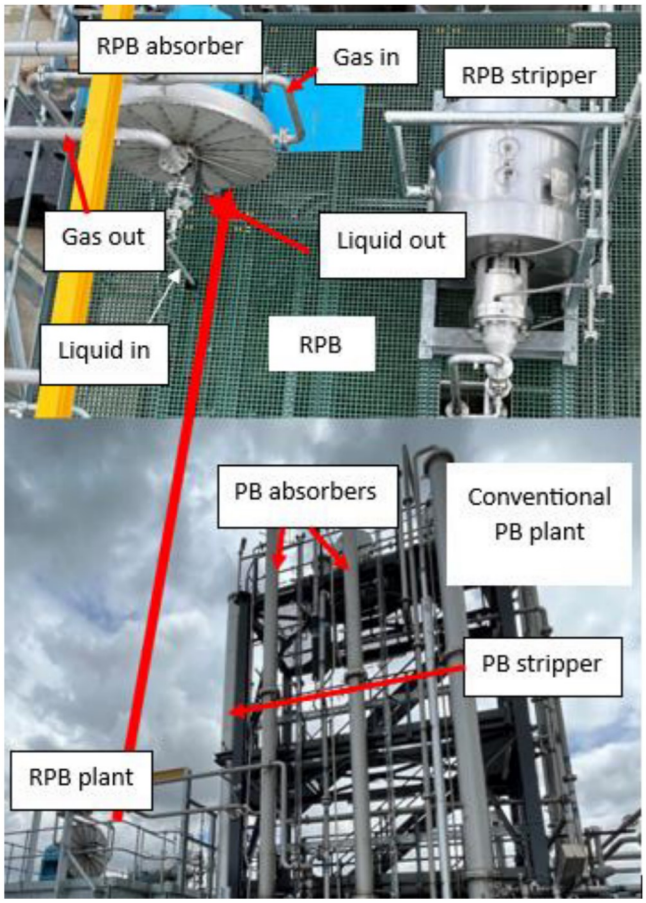

Figure 1: TERC RPB and PB CO_2 capture plants

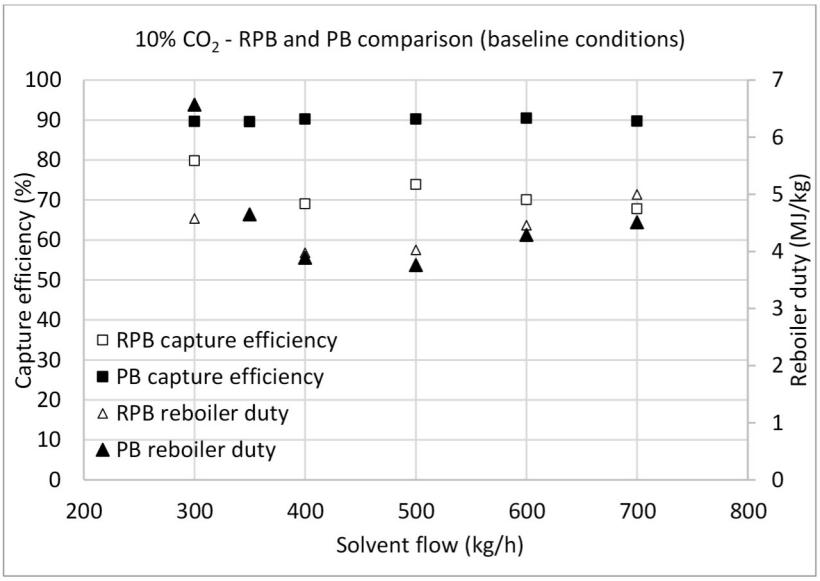

Figure 2: RPB and PB captrue efficiency and reboiler duty comparison (baseline condition, 10% CO_2)

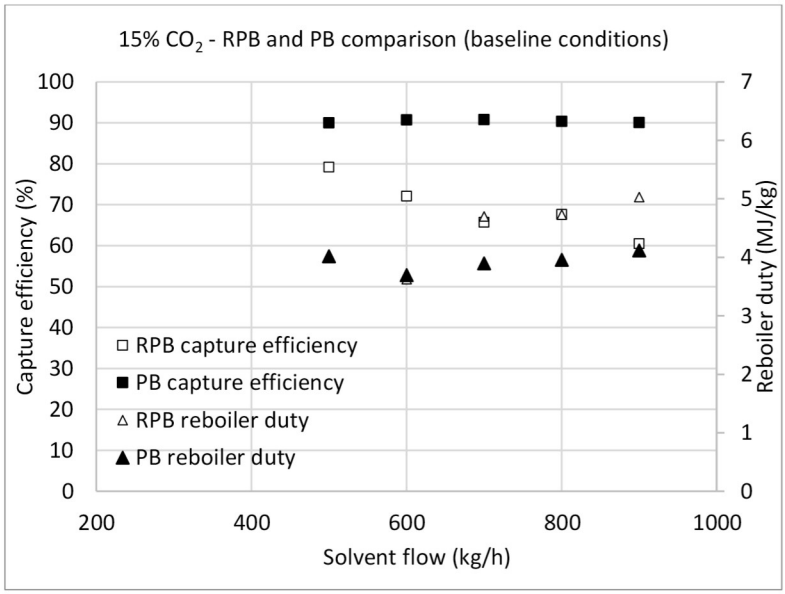

Figure 3: RPB and PB captrue efficiency and reboiler duty comparison (baseline condition, 15% CO_2)

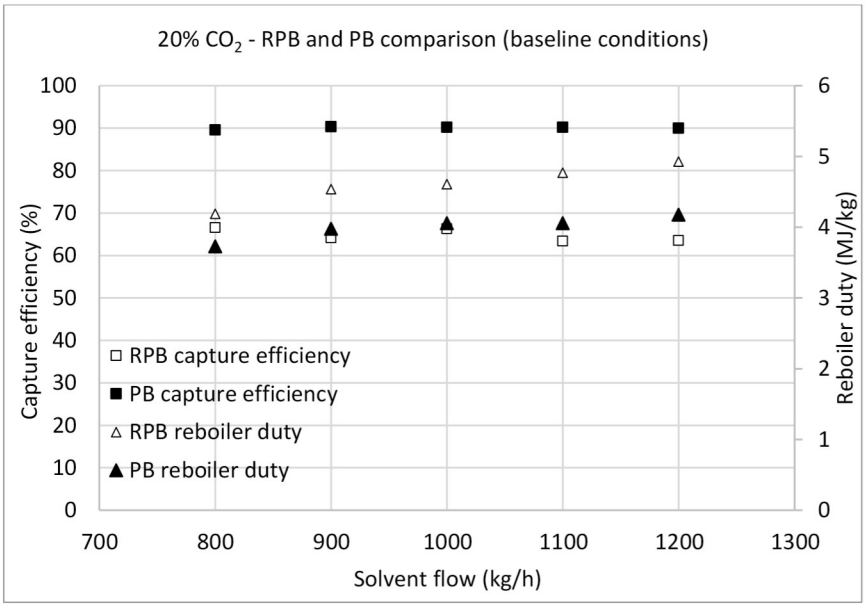

Figure 4: RPB and PB captrue efficiency and reboiler duty comparison (baseline condition, 20% CO_2)

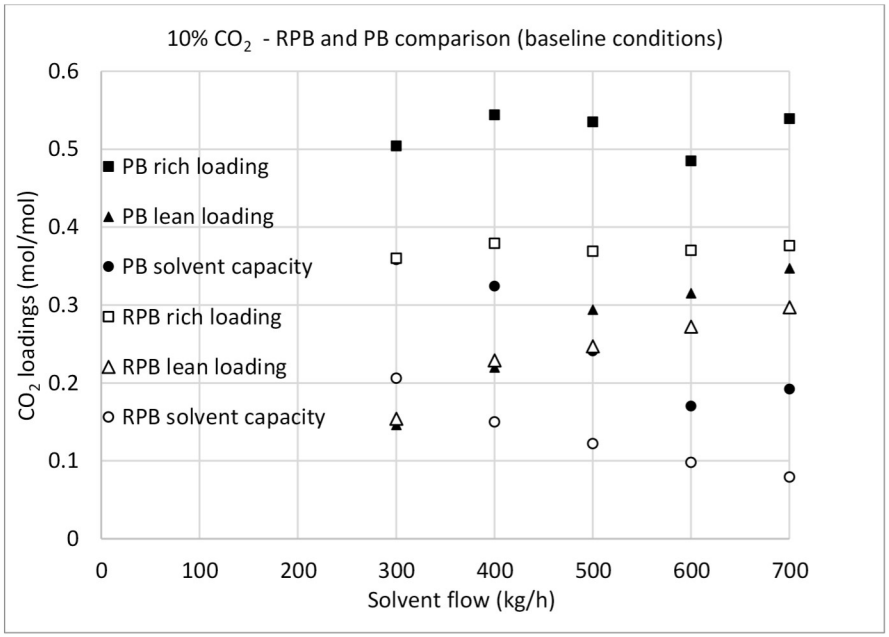

Figure 5: RPB and PB loadings comparison (baseline conditions, 10% CO_2)

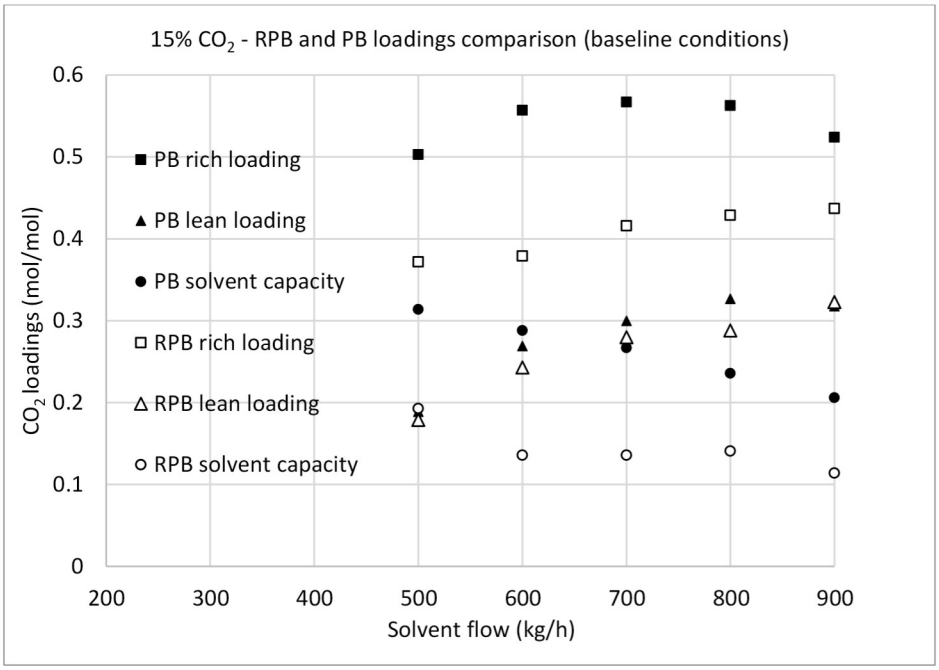

Figure 6: RPB and PB loadings comparison (baseline conditions, 15% CO_2)

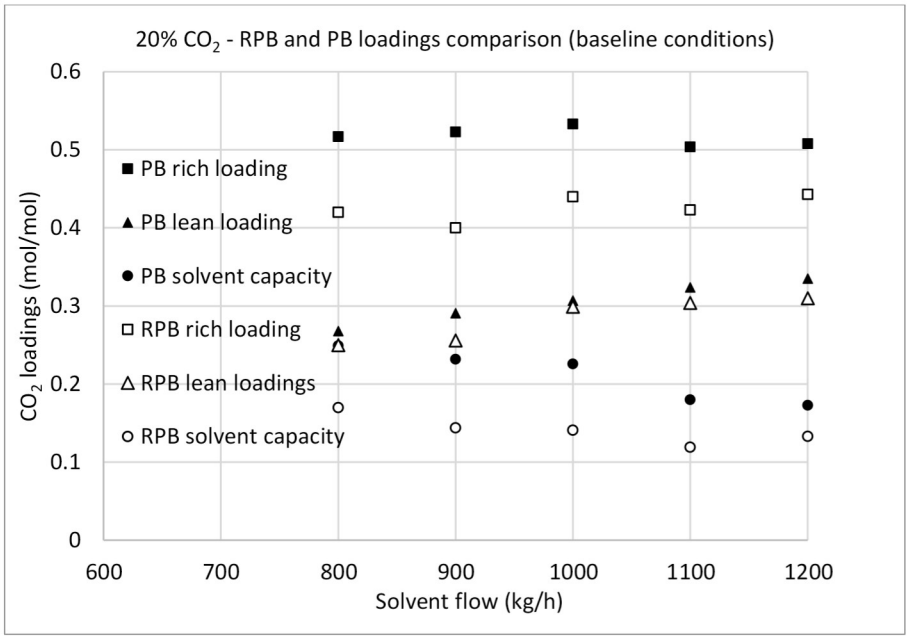

Figure 7: RPB and PB loadings comparison (baseline conditions, 20% CO_2)

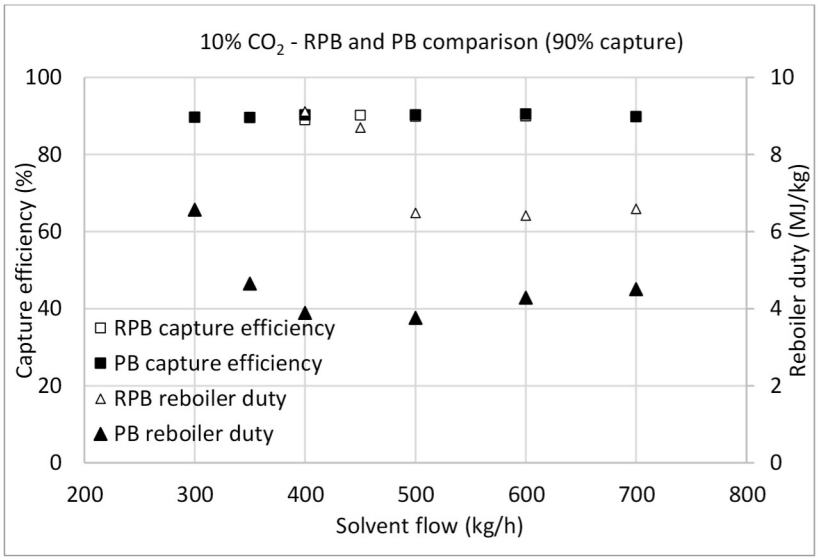

Figure 8: RPB and PB captrue efficiency and reboiler duty comparison (90% capture conditions, 10% CO_2)

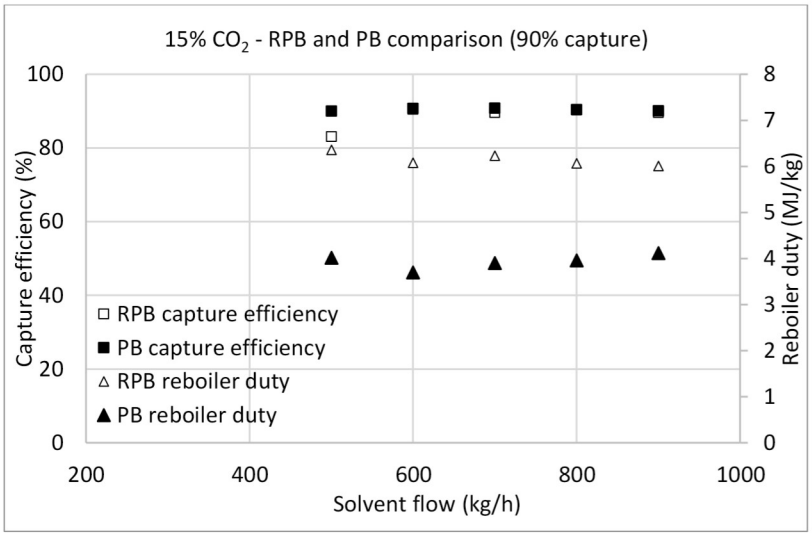

Figure 9: RPB and PB captrue efficiency and reboiler duty comparison (90% capture conditions, 15% CO_2)

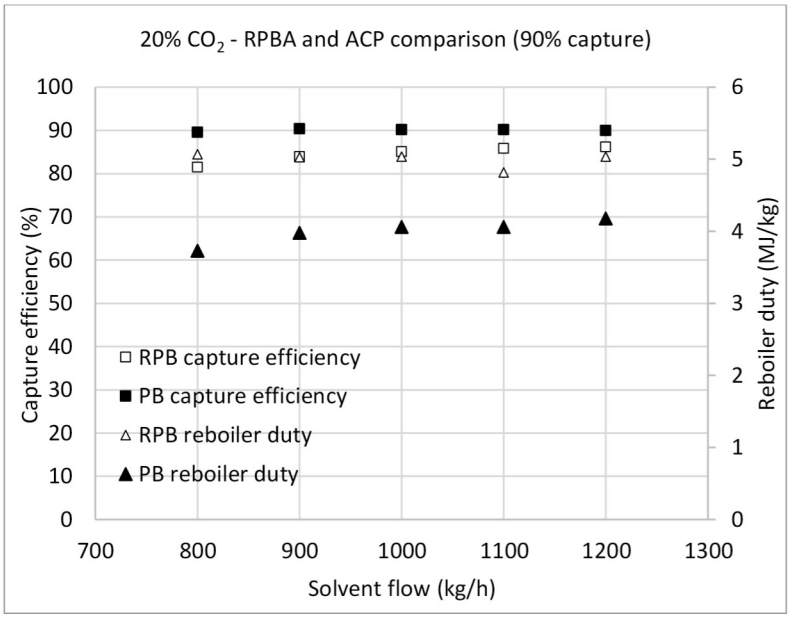

Figure 10: RPB and PB captrue efficiency and reboiler duty comparison (90% capture conditions, 20% CO_2)

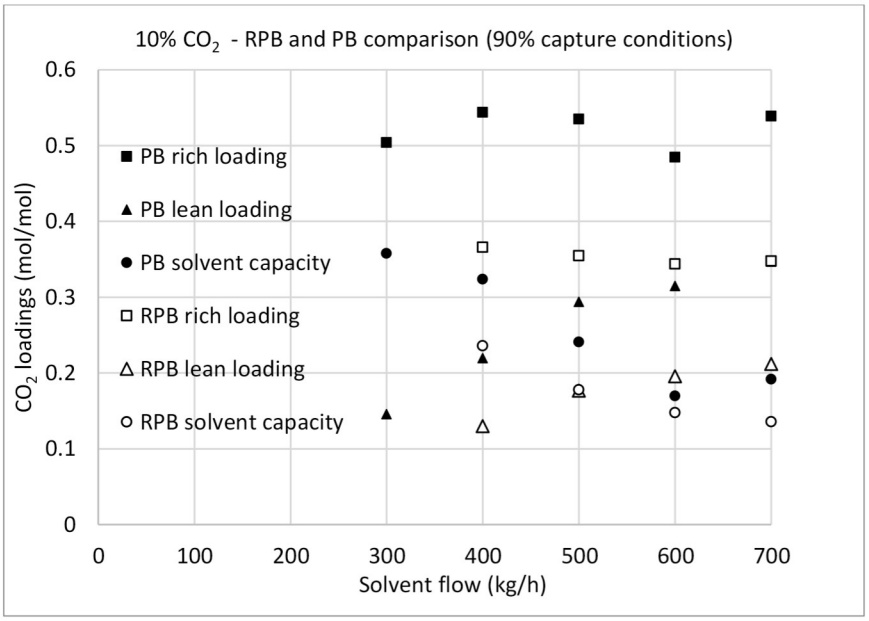

Figure 11: RPB and PB loadings comparison (90% capture conditions, 10% CO_2)

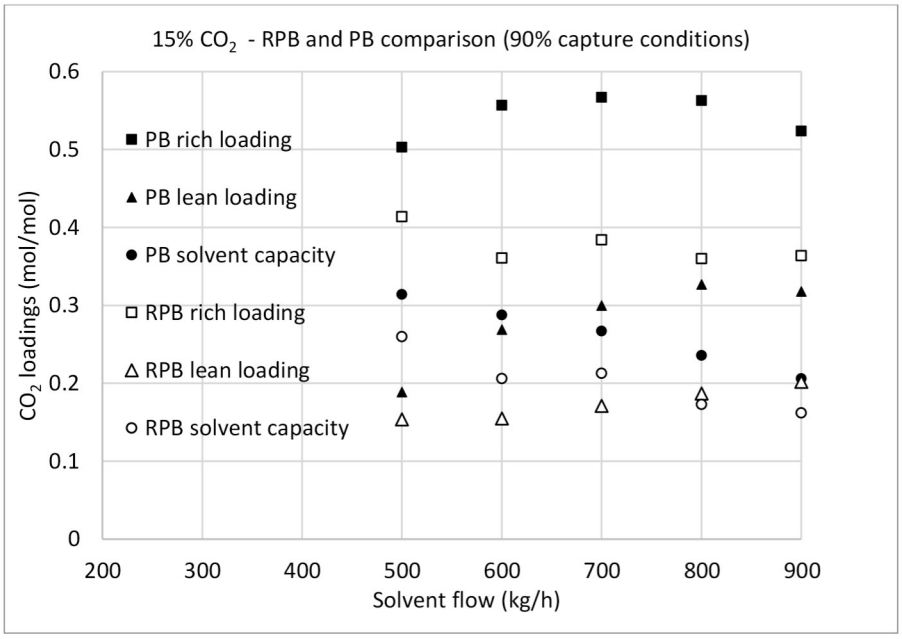

Figure 12: RPB and PB loadings comparison (90% capture conditions, 15% CO_2)

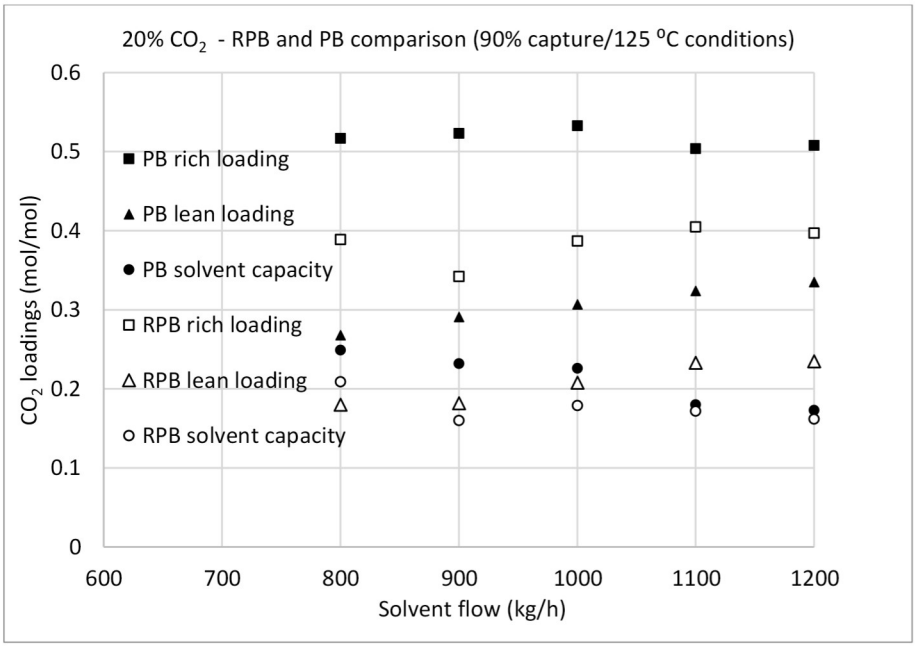

Figure 13: RPB and PB loadings comparison (90% capture conditions, 20% CO_2)

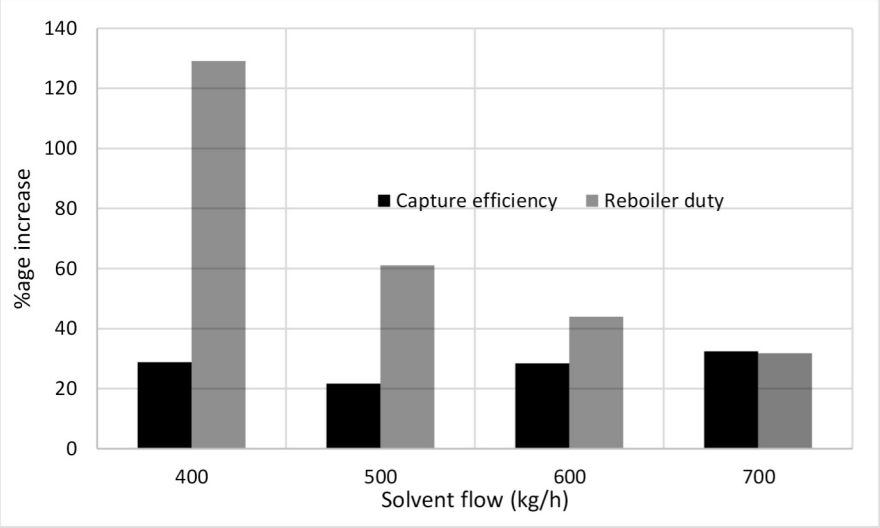

Figure 14: Percentage increase in the capture efficiency and reboiler duty with the RPB at 90% capture conditions wrt the baseline at 10% CO_2

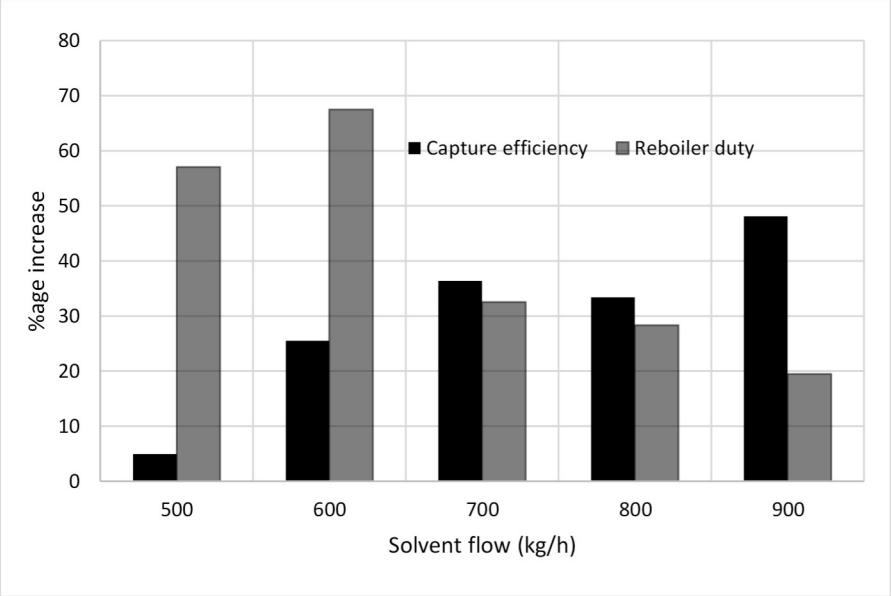

Figure 15: Percentage increase in the capture efficiency and reboiler duty with the RPB at 90% capture conditions wrt the baseline at 15% CO_2

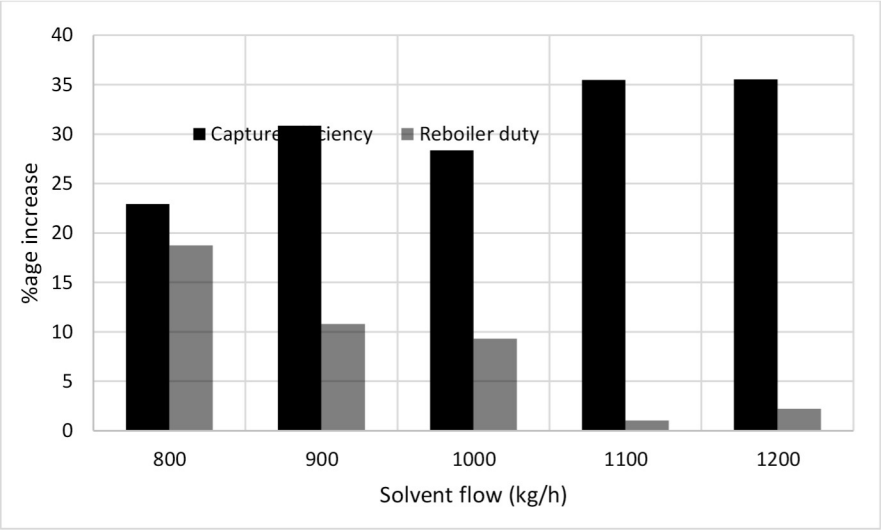

Figure 16: Percentage increase in the capture efficiency and reboiler duty with the RPB at 125 ^{o}C wrt the baseline at 20% CO_2

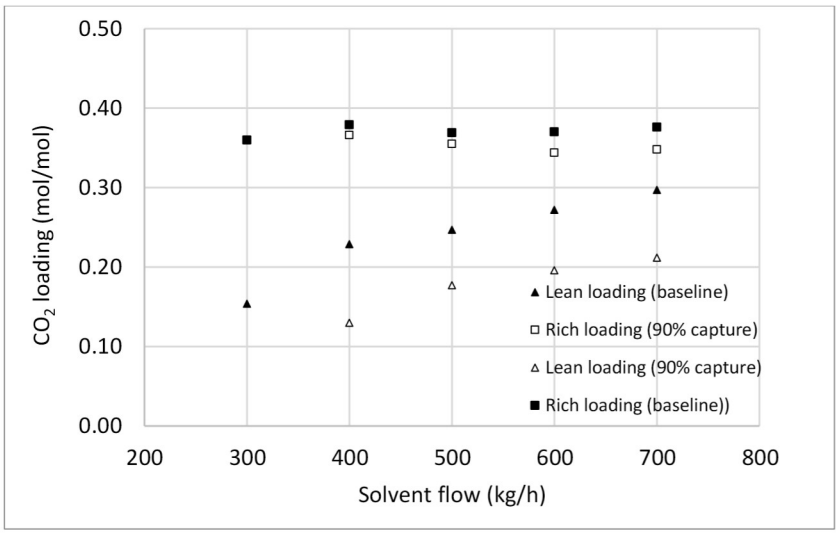

Figure 17: RPB loadings comparison (baseline and 90% capture conditions, 10% CO_2)

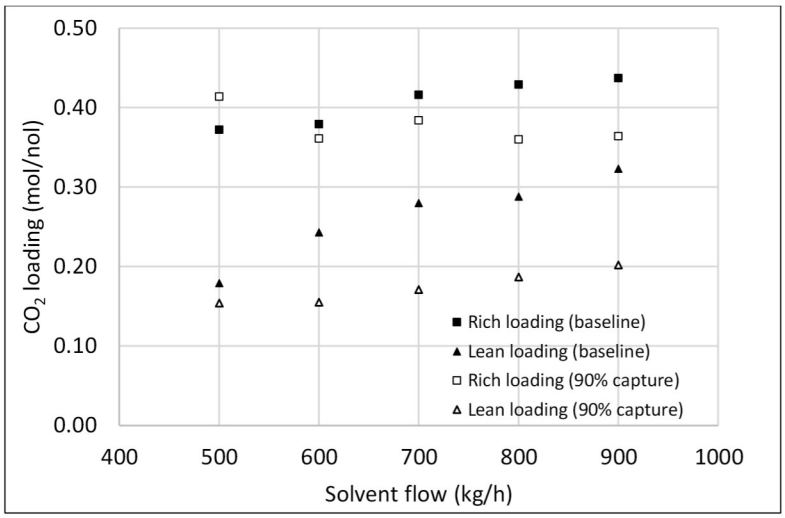

Figure 18: RPB loadings comparison (baseline and 90% capture conditions, 15% CO_2)

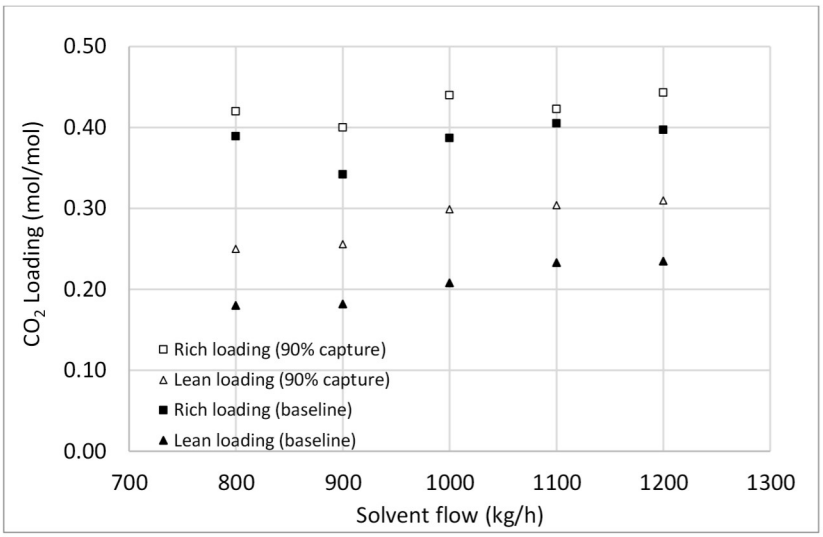

Figure 19: RPB loadings comparison (baseline and 90% capture conditions, 20% CO_2)

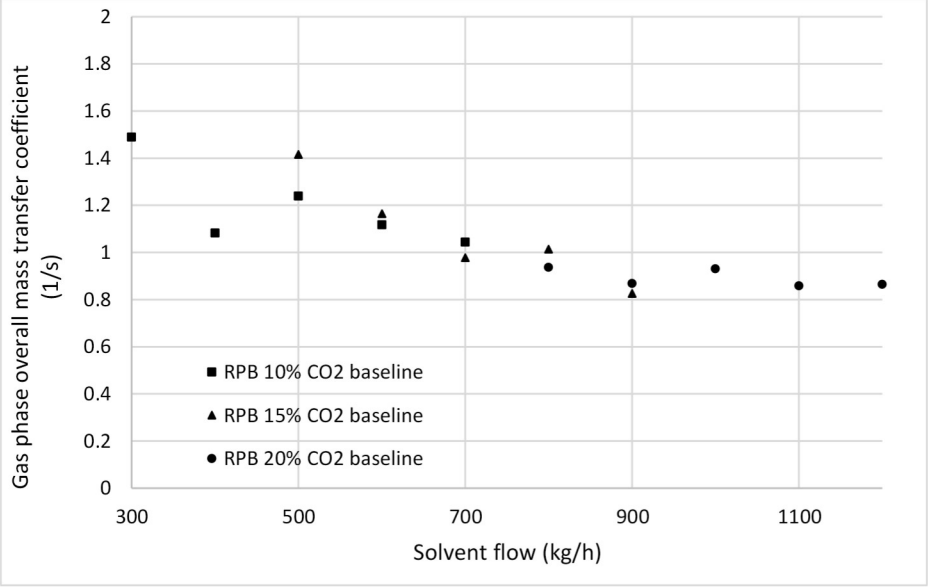

Figure 20: Overall gas phase mass transfer coefficient vs solvent flow

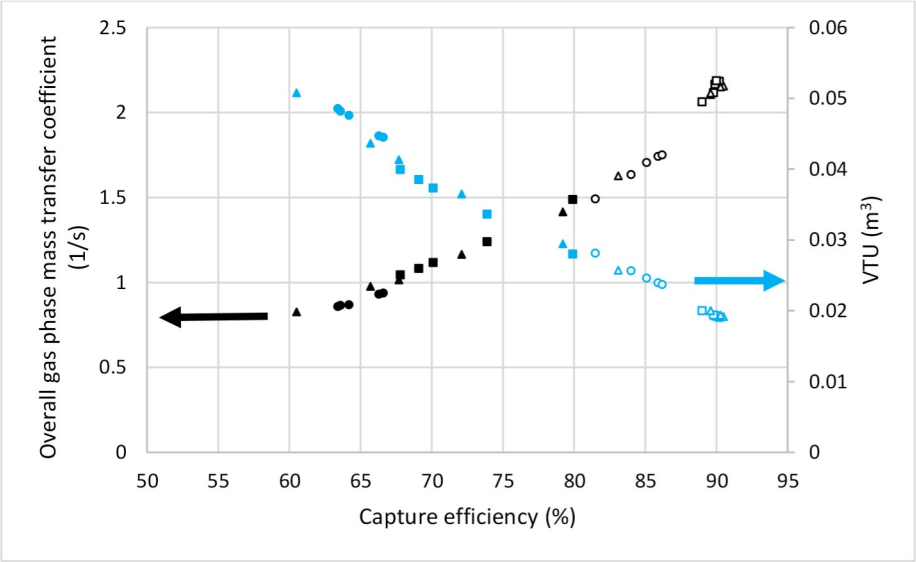

Figure 21: Capture efficiency vs VTU and overall gas phase mass transfer coefficient

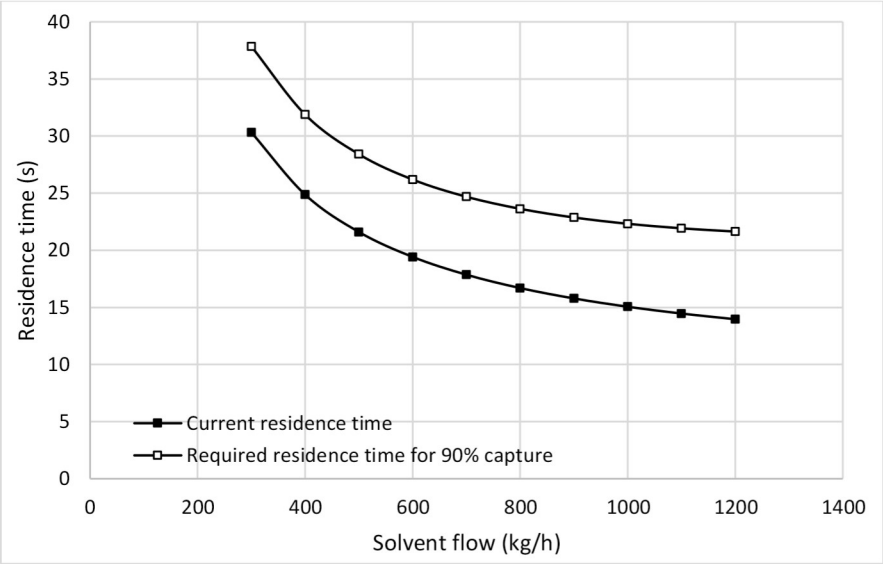

Figure 23: Solvent flow vs residence time in the RPB

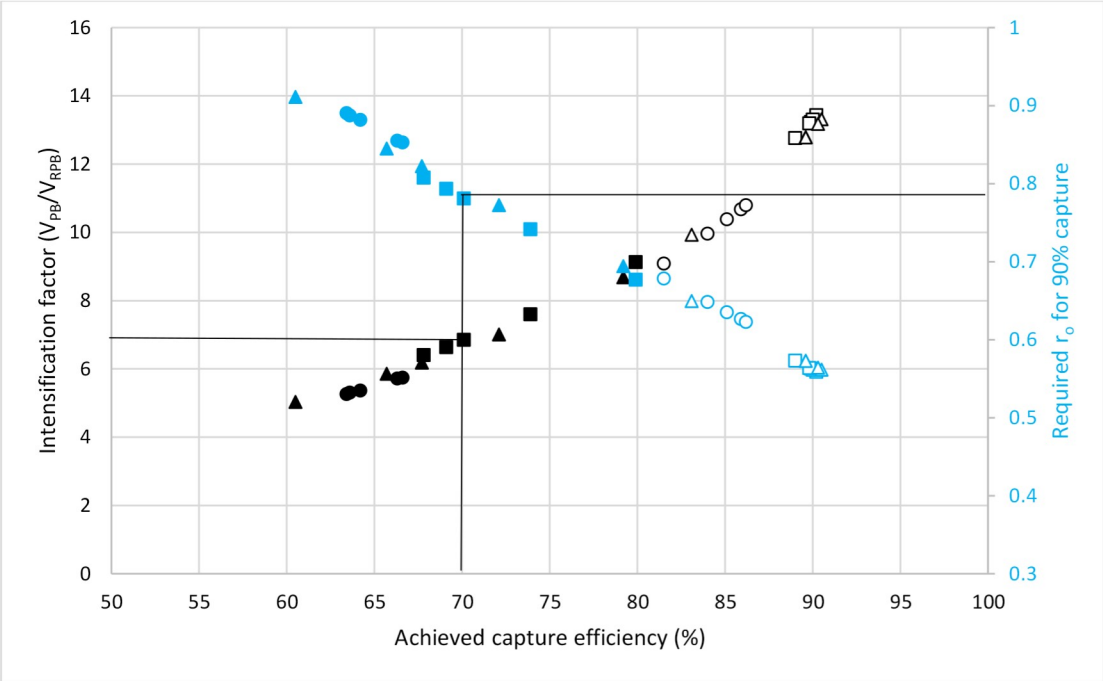

Figure 24: Capture efficiency vs required r_o and Intensification factor to achieve 90% capture